Available online at www.sciencedirect.com
SCIENCE DIRECT
Catalysis Today 114 (2006) 64–71
CATALYSIS TODAY
www.elsevier.com/locate/cattod

A novel Pd/MgAlO$_x$ catalyst for NO$_x$ storage-reduction

B.A. Silletti, R.T. Adams, S.M. Sigmon, A. Nikolopoulos, J.J. Spivey [1], H.H. Lamb *

Department of Chemical and Biomolecular Engineering, North Carolina State University Raleigh, NC 27695-7905, United States

Available online 20 March 2006

Abstract

A novel NO$_x$ storage-reduction catalyst consisting of Pd dispersed on a magnesium–aluminum oxide (MgAlO$_x$) support is described. The MgAlO$_x$ support was prepared from a synthetic Mg/Al layered double hydroxide, and Pd bis-acetylacetonate (acac) was adsorbed onto the freshly calcined support from toluene. The Pd/MgAlO$_x$ catalyst was pretreated in either O$_2$ or H$_2$ at 500 °C to decompose the adsorbed [Pd(acac)$_2$] and remove organic residues. NO$_x$ adsorption experiments were conducted at 300 °C using two gas mixtures: 500 ppm NO$_2$, 6% O$_2$ and 10% CO$_2$ (bal. He) and 500 ppm NO, 500 ppm N$_2$ and 5% O$_2$ (bal. He). Temperature-programmed desorption (TPD) and diffuse-reflectance infrared Fourier transform spectroscopy (DRIFTS) evidence that NO$_2$ adsorption on MgAlO$_x$ produces primarily surface nitrate species. The adsorption capacity of the support for NO + O$_2$ is four-fold lower than for NO$_2$. Temperature-programmed reduction (TPR) in flowing H$_2$ demonstrates that surface nitrate and nitrite species on MgAlO$_x$ are reduced to N$_2$ at 300–400 °C. The adsorption capacity of Pd/MgAlO$_x$ for NO + O$_2$ is almost four-fold greater than MgAlO$_x$ evidencing a catalytic role of Pd in the NO$_x$ storage mechanism. TPR in flowing H$_2$ indicates that the adsorbed NO$_x$ species are removed at very low temperatures (~50 °C) suggesting that they are located near the catalytically active Pd sites.

Keywords: NO$_x$ adsorption; Palladium; Hydrotalcite; Temperature-programmed desorption (TPD); Temperature-programmed reduction (TPR); DRIFTS; X-ray photoelectron spectroscopy (XPS)

1. Introduction

Increasingly stringent environmental regulations for diesel engines and the automotive industry's shift toward lean-burn gasoline engines provide the impetus for new approaches to NO$_x$ emission control. While conventional three-way exhaust catalysts are effective under stoichiometric exhaust conditions, reducing NO$_x$ emissions under lean (oxygen-rich) conditions requires new catalytic technology [1]. The NO$_x$ storage-reduction (NSR) catalyst or NO$_x$ trap is one promising candidate [2]. The prototypical NSR catalyst, Pt/BaO/Al$_2$O$_3$, consists of Pt and BaO dispersed on a high-surface-area alumina support [3]. The NSR catalyst adsorbs NO$_x$ compounds under lean conditions and is regenerated periodically under rich conditions releasing N$_2$, H$_2$O and CO$_2$. The surface properties of the alkaline earth metal oxide storage component and the noble metal catalyst are critical to the efficacy of the device [3–5]. The commercial viability of NSR catalysts is limited by the narrow range of operating temperatures, thermal degradation and deactivation by sulfur adsorption [6,7].

This paper describes the preparation, characterization and testing of a NSR catalyst consisting of Pd dispersed on a strongly basic magnesium–aluminum oxide (MgAlO$_x$) support that also functions as a NO$_x$ adsorbent. This research was motivated by recent results suggesting that a Pd/MgAlO$_x$ catalyst could offer potential advantages over Pt/BaO/Al$_2$O$_3$. Salasc et al. found that Pd/BaO/Al$_2$O$_3$ exhibited greater low-temperature NO$_x$ storage capacity than Pt/BaO/Al$_2$O$_3$ despite the lower NO oxidation activity of the supported Pd catalyst [8]. Moreover, Fornasari et al. reported that Pt and Pt–Cu dispersed on a hydrotalcite-derived MgAlO$_x$ support showed greater NO$_x$ storage capacity at 200 °C and better sulfur tolerance than Pt/BaO/Al$_2$O$_3$ [9]. Hydrotalcite is an anionic clay with the ideal formula: Mg$_6$Al$_2$(OH)$_{16}$CO$_3$·4H$_2$O. Hydrotalcite-like compounds are layered double hydroxides (LDH) with the general formula $[M^{2+}_{1-x}M^{3+}_{x}(OH)_2]^{+}[A^{n-}_{x/n}]\cdot mH_2O$, where x is the $M^{3+}/(M^{2+} + M^{3+})$ ratio, and they consist of positively charged brucite-like layers separated by negatively charged layers of anions and water [10]. LDH are readily synthesized and highly customizable for a variety of catalytic applications, and mixed oxides derived by thermal decomposition of synthetic Mg/Al

* Corresponding author. Tel.: +1 919 515 6395; fax: +1 919 515 3465.
E-mail address: lamb@ncsu.edu (H.H. Lamb).
[1] Present address: Department of Chemical Engineering, Louisiana State University, Baton Rouge, LA, United States.

0920-5861/$ – see front matter
doi:10.1016/j.cattod.2006.02.003

LDH contain Al^{3+} Lewis acid sites in addition to strongly basic sites like those characteristic of MgO [11].

The $Pd/MgAlO_x$ catalyst was prepared by adsorption of Pd bis-acetylacetonate [$Pd(acac)_2$] onto the calcined support from toluene solution. The use of a non-aqueous, halide-free preparation method is critical to avoid reconstruction of the LDH structure and modification of the acid–base properties of the support. $Pd/MgAlO_x$ catalysts prepared by Prinetto et al. following a similar procedure were found to contain isolated Pd atoms and/or very small Pd^0 clusters [12]. NO_2 adsorption and $NO + O_2$ adsorption were investigated on the $Pd/MgAlO_x$ catalyst and $MgAlO_x$ support using temperature-programmed desorption (TPD) and temperature-programmed reduction (TPR). The adsorbed species produced by NO_2 adsorption on $MgAlO_x$ were characterized by diffuse-reflectance infrared Fourier transform spectroscopy (DRIFTS). The $Pd/MgAlO_x$ catalyst was characterized by Pd 3d X-ray photoelectron spectroscopy (XPS) after selected treatments.

2. Experimental methods

2.1. Materials

Ultra-high purity He and H_2, extra-dry O_2 and three certified gas mixtures: 1000 ppm NO_2, 20% CO_2 and 12% O_2 (bal. He); 1000 ppm NO and 1000 ppm N_2 (bal. He); and 1000 ppm O_2 and 1000 ppm N_2 (bal. He) were supplied by National Welders. Toluene (ACS reagent) was obtained from Fisher Scientific and used without further purification. A synthetic LDH powder with a Mg:Al ratio of 7:3 was obtained from a commercial source and calcined in flowing O_2 at 600 °C.

2.2. Catalyst preparation

[$Pd(acac)_2$] was adsorbed from toluene solution onto freshly calcined $MgAlO_x$ support in a N_2-filled mBraun glovebox. After stirring overnight, a light-yellow solid was recovered by filtration and dried for 5 h on a vacuum line. The dried $Pd/MgAlO_x$ catalyst was transferred to a vial and stored in a desiccator. A Pd loading of 1.34 wt% was determined by Galbraith Laboratories using ICP-OES analysis.

2.3. Catalyst testing

TPD and TPR experiments were performed in a tubular quartz micro-reactor with continuous on-line sampling using a quadrupole mass analyzer (QMA) [13]. The QMA signals at mass-to-charge (m/z) ratios of 2(H_2), 4(He), 18(H_2O), 28(N_2 and CO), 30 (NO), 32(O_2), 44(CO_2 and N_2O) and 46(NO_2) were monitored during each experiment, and these were recorded together with the temperature by a PC. Catalyst samples (0.3 g) were loaded into a fritted quartz tube, and the tube was installed in a vertical split-tube furnace with a Type K thermocouple located near the center of the catalyst bed. Prior to NO_x adsorption, the $Pd/MgAlO_x$ catalyst was pretreated in either flowing H_2 or flowing 20% O_2 at 500 °C for 1 h; the $MgAlO_x$ support was degassed in flowing He at 500 °C for 1 h. NO_x adsorption experiments were conducted at 300 °C using two gas compositions: 500 ppm NO_2, 6% O_2 and 10% CO_2 (bal. He); 500 ppm NO, 500 ppm N_2 and 5% O_2 (bal. He). These compositions were generated by blending certified gas mixtures with He and/or O_2 using calibrated rotameters. The total gas flow rate during adsorption was 100 sccm. After 30 min exposure to NO_x, samples were purged with He and cooled to approximately 50 °C. TPD and TPR experiments were performed using a linear temperature ramp of 10 °C/min from ~50 to 600 °C. The He (TPD) and H_2 (TPR) flow rates were 25 sccm each. Samples were purged with He at 500 °C for at least 30 min after TPR.

2.4. Catalyst characterization

The X-ray diffraction (XRD) pattern of the calcined LDH was recorded using a INEL XRG 3000 with a CPS 120 detector and a Ge crystal monochromator. The X-ray source was a fine-focused Cu tube operated at 30 mA and 34.8 kV. Specific surface areas were determined by N_2 adsorption at 77 K using a Micromeritics Flow Sorb II 2300 instrument.

XPS samples were pretreated in a quartz micro-reactor tube, sealed and unloaded in a N_2-filled mBraun glovebox. The catalyst powder was pressed into a thin self-supporting disk which was attached to a Mo sample holder using double-sided Cu tape. The sample holder was transported and inserted into the load lock of the surface analysis chamber under N_2. XP spectra were measured using a PHI 3057 spectrometer comprising a 10–360 spherical capacitor analyzer, Omni Focus III fixed-aperture lens, 16-element multichannel detector and 257 DR11 PC interface card. The Mg anode of a PHI 1248 dual-anode (Mg/Al) X-ray source was used. A photoelectron take-off angle of 45° with respect to the surface normal was employed. The Pd 3d binding energies are referenced to the C 1s peak of adventitious carbon at 284.8 eV.

DRIFTS experiments were conducted using an Analect RFX-65 FTIR spectrometer equipped with a Harrick Praying Mantis accessory, a high-temperature in situ DRIFTS cell and a high-sensitivity MCT detector. Spectra were recorded at 8 cm^{-1} resolution using 1024 interferometer scans for the background and 512 scans for the sample. Each spectrum was recorded using dehydrated KBr powder in He as the background. Ultra-high purity He and a certified gas mixture containing 1000 ppm NO_2, 20% CO_2 and 12% O_2 in balance He were metered using a rotameter. Approximately 50 mg of sample was placed in the sample cup, heated at 10 °C/min to 500 °C in flowing He (15 sccm), and soaked for 1 h. The sample was allowed to cool to 300 °C in flowing He, and a baseline DRIFTS spectrum was recorded. Subsequently, the sample was treated in the flowing NO_2 gas mixture (12 sccm) at 300 °C for 30 min and then purged in He (15 sccm) for 30 min. Spectra were recorded at 1, 5 and 30 min of adsorption of the mixed gas as well as 1, 5 and 30 min after purging in He. After the adsorption and purge, the sample was heated in flowing He for 30 min at 400 °C and at 500 °C.

3. Results and discussion

3.1. $MgAlO_x$

The specific surface area of the LDH-derived $MgAlO_x$ support is approximately 190 m^2/g, and its XRD pattern contains sharp Bragg diffraction peaks at 50.4, 73.8, 89.5 and 94.8° 2θ [14]. These peaks are indexed to a $MgAlO_x$ phase with a rocksalt crystal structure like MgO albeit with a smaller lattice parameter [15,16]. The smaller lattice parameter has been interpreted as evidence for Al^{3+} incorporation into the MgO lattice [15]. The XRD pattern gives no evidence of separate MgO and Al_2O_3 phases.

The TPD traces in Fig. 1a were recorded after a $MgAlO_x$ sample was exposed to a gas mixture containing 1000 ppm NO_2, 20% CO_2 and 12% O_2 (bal. He) at 300 °C for 30 min. Large symmetric peaks due to concurrent desorption of NO ($m/z = 30$) and O_2 ($m/z = 32$) are observed at 475 °C. NO_2 was not detected as a desorption product even though the NO_2^+ parent ion ($m/z = 46$) had been observed using the same gas inlet system and QMA in TPD experiments on other NSR catalysts [14]. A small contribution to the $m/z = 30$ signal from dissociative ionization of NO_2 cannot be excluded; however, fragmentation of NO_2 to O_2^+ ($m/z = 32$) via electron impact ionization can be neglected. Calibration of the QMA intensities indicates that the NO/O_2 ratio from TPD is approximately 4/3, as expected for the stoichiometric decomposition of surface nitrate species:

$$2NO^-_{3(s)} \rightarrow O^{2-}_{(s)} + 2NO + \tfrac{3}{2}O_2 \quad (1)$$

A small symmetric CO_2 TPD peak is observed at 330 °C, and this peak is assigned to CO_2 adsorbed on strongly basic sites [17]. From the calibrated areas of the TPD peaks, we estimate that the NO_2 adsorption capacity of the $MgAlO_x$ is 12.3 μmol/g at 300 °C (Table 1); however, the capacity may be somewhat higher in the absence of co-adsorbed CO_2.

Table 1
NO_x adsorption on $MgAlO_x$ and $Pd/MgAlO_x$

Catalyst	Pretreatment	Species adsorbed	NO uptake (μmol/g)	NO TPD (μmol/g)	NO/O_2 TPD
$MgAlO_x$	Degas	NO_2[a]	–	12.3	1.32
	Degas	NO/O_2[b]	9.4	3.1	1.86
$Pd/MgAlO_x$	TPO	NO_2[c]	–	20.8	1.10
	TPR	NO_2[c]	–	14.5	1.80
	TPD	NO_2[c]	–	16.7	1.54
$Pd/MgAlO_x$	TPO	NO/O_2[b]	28.1	11.1	1.25
	TPR	NO/O_2[b]	61.7	20.7	1.46
	TPD	NO/O_2[b]	36.6	11.4	1.30

[a] 1000 ppm NO_2, 12% O_2 and 20% CO_2 (bal. He).
[b] 500 ppm NO, 500 ppm N_2 and 5% O_2 (bal. He).
[c] 500 ppm NO_2, 6% O_2 and 10% CO_2 (bal. He).

The DRIFT difference spectra in Fig. 2 were recorded during exposure of a $MgAlO_x$ sample to a gas mixture containing 1000 ppm NO_2, 20% CO_2 and 12% O_2 (bal. He) at 300 °C and during subsequent heating in flowing He at 300, 400 and 500 °C. The strong bands at 1600, 1380 and 1075 cm^{-1} that are observed under the gas mixture are assigned to monodentate surface carbonate species [17]. These bands diminish markedly after purging with He at 300 °C and are virtually eliminated after heating in He at 400 °C, consistent with the CO_2 desorption trace in Fig. 1a. The bands at 1540, 1280 and 1050 cm^{-1} that remain after purging with He at 400 °C are associated with NO_x species.

Band assignments in the 1700–1000 cm^{-1} region are complicated by overlap of various N–O stretching modes. The free

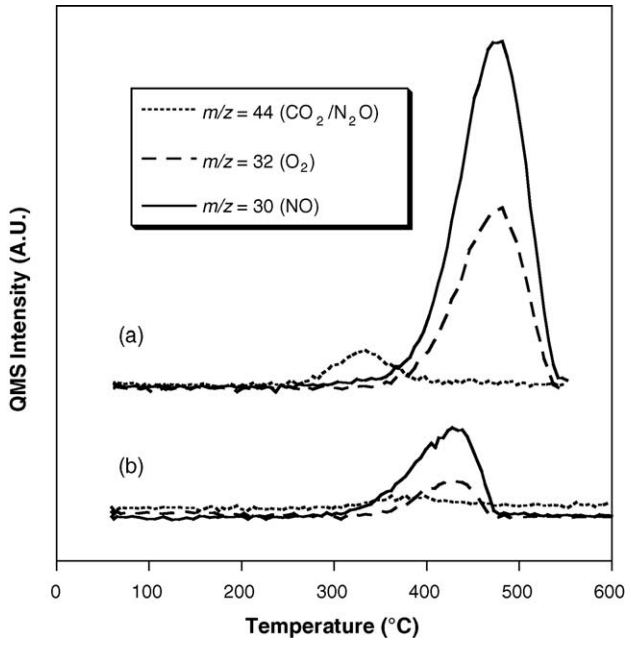

Fig. 1. TPD traces recorded after exposure of $MgAlO_x$ to NO_2 (a) and NO + O_2 (b) at 300 °C for 30 min.

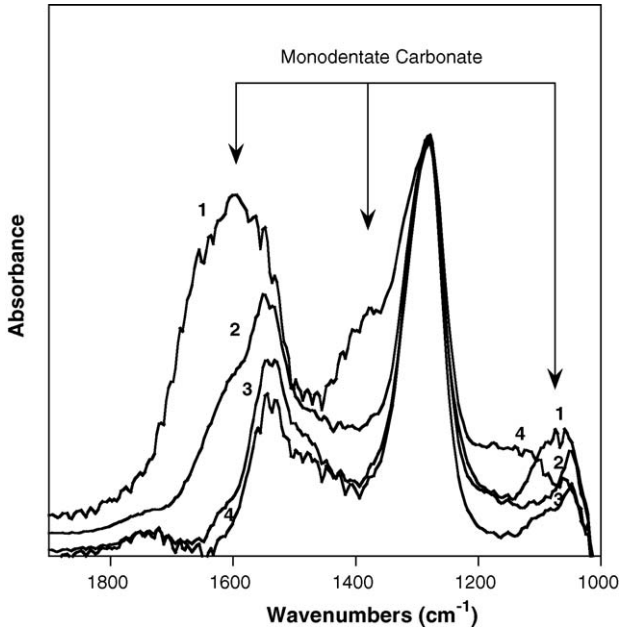

Fig. 2. DRIFT difference spectra recorded during exposure of $MgAlO_x$ to a gas mixture containing 1000 ppm NO_2, 20% CO_2 and 12% O_2 at 300 °C (1) and during subsequent heating in flowing He at 300 °C (2), 400 °C (3) and 500 °C (4).

nitrate ion (NO_3^-, D_{3h} symmetry) exhibits a single infrared-active mode at 1380 cm^{-1}. Monodentate surface nitrate species exhibit 3 infrared bands at 1530–1480, 1290–1250 and 1035–970 cm^{-1}; analogous bands appear at 1565–1500, 1300–1260 and 1040–1010 cm^{-1} for bidentate (chelating) surface nitrate species [18]. By comparison, we assign the strong band at 1540 cm^{-1} and the shoulder at 1480 cm^{-1} to surface nitrate species in chelating bidentate and monodentate coordination to surface metal cations, respectively. The intensities of these spectral features decrease as the sample is heated from 300 to 500 °C in He. Concurrently, the band at 1050 cm^{-1} also decreases in intensity. Thus, it is reasonable to associate the NO and O_2 TPD peaks in Fig. 1a primarily with the decomposition of surface nitrate species. Surface nitrate species are expected to exhibit an additional $\nu_{as}(NO_2)$ infrared band in the 1250–1300 cm^{-1} region. Apparently, these bands are obscured by the very strong band at 1280 cm^{-1} which does not respond to thermal treatment. We speculate that this band may arise from bulk nitrite species associated with Al^{3+} ions, since an analogous band is not observed after NO_2 adsorption on MgO [14]. The free nitrite ion (NO_2^-, C_{2v} symmetry) exhibits infrared-active symmetric and antisymmetric stretching bands at 1330 and 1260 cm^{-1}.

The TPD traces in Fig. 1b were recorded after a $MgAlO_x$ sample was exposed to a gas mixture containing 500 ppm NO, 500 ppm N_2 and 5% O_2 (bal. He) at 300 °C for 30 min. Asymmetric TPD peaks due to concurrent desorption of NO and O_2 are observed at approximately 430 °C. In comparison to Fig. 1a, the NO peak area is approximately a factor of 4 smaller and the NO/O_2 ratio (1.86) is significantly higher indicating a lower surface coverage and a different stoichiometry for the adsorbed NO_x species. The variable stoichiometry of adsorbed NO_x species on alkaline earth oxides and Al_2O_3 has been attributed to mixtures of nitrite and nitrate surface species [19,20]. Theoretical studies suggest that cooperative adsorption of NO and NO_2 on MgO(0 0 1) leads to the formation of surface nitrite–nitrate pairs [21]. Provided that NO_2 desorption can be neglected, thermal decomposition of NO_3^-/NO_2^- pairs

$$NO^-_{2(s)} + NO^-_{3(s)} \rightarrow O^{2-}_{(s)} + 2NO + O_2 \quad (2)$$

is expected to yield in an NO/O_2 ratio of 2:1—in better agreement than Eq. (1) with the TPD data for NO + O_2 adsorption on $MgAlO_x$.

The TPR traces in Fig. 3a were recorded after a $MgAlO_x$ sample was exposed to a gas mixture containing 1000 ppm NO_2, 20% CO_2 and 12% O_2 (bal. He) at 300 °C for 30 min. The data show the evolution of nitrogen-containing products during heating in flowing H_2 at 10 °C/min. Relatively broad N_2O and N_2 peaks are observed at 300 and 350 °C, respectively. There is a low-temperature shoulder on the N_2 peak that corresponds closely in temperature to the N_2O peak. We infer that these products result from reduction of surface nitrate species, since the coupled NO and O_2 desorption peaks due to thermal decomposition of surface nitrate species are absent. The TPR traces in Fig. 3b were recorded after a $MgAlO_x$ sample was exposed to a gas mixture containing

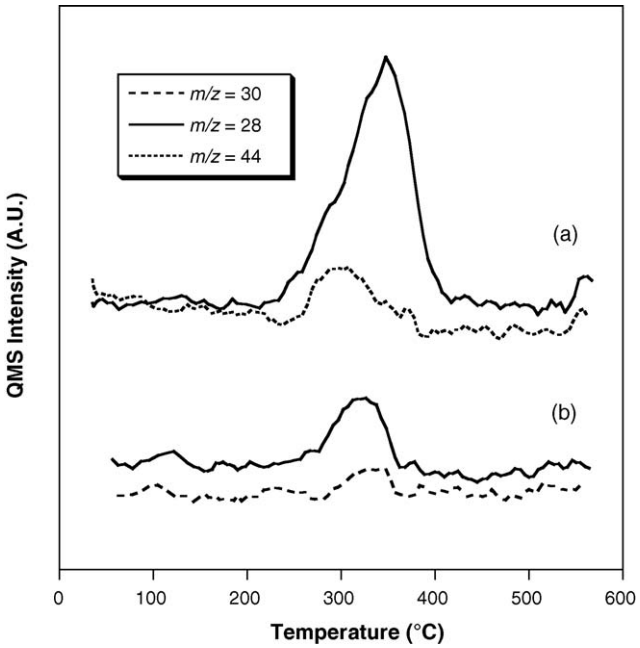

Fig. 3. TPR traces recorded after exposure of $MgAlO_x$ to NO_2 (a) and NO + O_2 (b) at 300 °C for 30 min.

500 ppm NO, 500 ppm N_2 and 5% O_2 (bal. He) at 300 °C for 30 min. In this case, N_2 and NO peaks are observed at 320 and 330 °C, respectively. In comparison to Fig. 3a, the N_2 peak area is significantly smaller, as expected given the lower NO + O_2 adsorption capacity of $MgAlO_x$. N_2 is the major reduction product regardless of whether $MgAlO_x$ was exposed to NO_2 or NO + O_2; however, the minor product shifts from N_2O in the former case to NO in the latter.

3.2. *Pd/MgAlO$_x$*

The Pd 3d XP spectra of the Pd/$MgAlO_x$ catalyst after selected treatments are shown in Fig. 4. The Pd $3d^{3/2}$ and $3d^{5/2}$ spin–orbit doublet appears on the right in each spectrum; the large feature on the left is associated with the $MgAlO_x$ support. The XP spectrum (Fig. 4a) of the Pd/$MgAlO_x$ catalyst after reduction in flowing H_2 at 500 °C for 1 h consists of a relatively well-resolved Pd 3d doublet, and the electron binding energy (E_b) of the $3d^{5/2}$ peak (335.0 eV) is indicative of metallic Pd. Prinetto et al. reported that similarly prepared Pd/$MgAlO_x$ samples contain isolated Pd^0 atoms and/or very small Pd clusters based on high-resolution transmission electron microscopy and FTIR spectroscopy of chemisorbed CO [12]. The XP spectrum (Fig. 4b) of the Pd/$MgAlO_x$ catalyst after pretreatment in flowing O_2 at 500 °C for 1 h is indicative of predominantly Pd^{2+} species (E_b = 336.3 eV). The Pd 3d peaks, however, are broadened suggesting that there may be minor contributions from other Pd oxidation states. The local chemical bonding and state of aggregation of the supported Pd(II) oxo species, however, cannot be established from these data.

The TPD traces in Fig. 5a were recorded after an oxygen-pretreated Pd/$MgAlO_x$ catalyst was exposed to a gas mixture

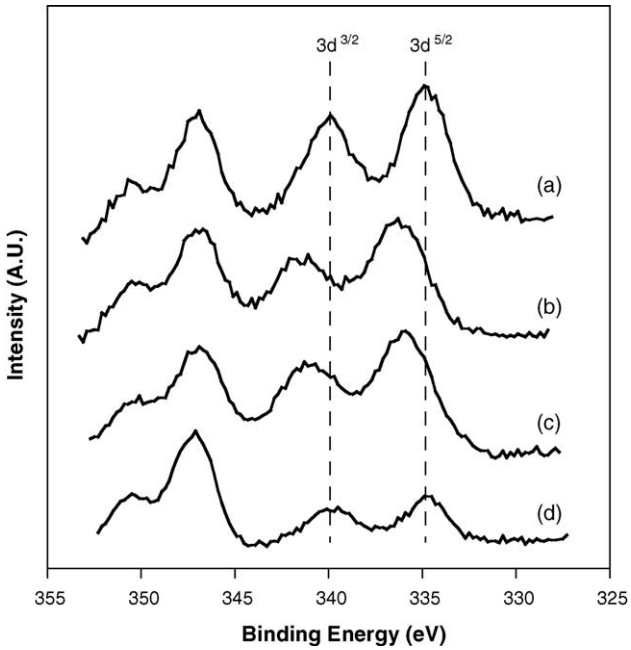

Fig. 4. Pd 3d XP spectra of Pd/$MgAlO_x$ catalyst: after pretreatment in flowing H_2 at 500 °C (a), after pretreatment in flowing O_2 at 500 °C (b), reduced catalyst after exposure to NO + O_2 at 300 °C for 30 min (c), and sample of (c) after heating to 600 °C in flowing He (d).

containing 500 ppm NO_2, 10% CO_2 and 6% O_2 (bal. He) at 300 °C for 30 min. Strong symmetric NO and O_2 desorption peaks are observed at 445 °C; however, the NO/O_2 ratio (1.10) is lower than expected for surface nitrate species on $MgAlO_x$. The CO_2 TPD peak near 300 °C is weak and broad in comparison to Fig. 1a; however, the peak areas are comparable indicating similar densities of strongly basic sites. (The additional CO_2 desorption peak near 100 °C is ascribed to weakly adsorbed CO_2 arising from incomplete purging of the reactor prior to cooling.) The NO_2 storage capacity of the oxygen-pretreated Pd/$MgAlO_x$ catalyst (Table 1) is 70% greater than the $MgAlO_x$ support indicating that the supported Pd oxo species provide additional sites for NO_2 adsorption. The higher NO_2 storage capacity and lower NO/O_2 TPD ratio observed for NO_2 adsorption on an oxygen-pretreated Pd/$MgAlO_x$ catalyst may result from the formation of surface nitrates by reaction with supported Pd oxo species:

$$PdO_{(s)} + NO_2 \rightarrow Pd(NO_3)_{(s)} \quad (3)$$

Thermal decomposition of the resulting surface Pd nitrate species to NO and O_2 (with concomitant Pd reduction) would yield an NO/O_2 ratio of 1. The rising O_2 signal between 500 and 600 °C in Fig. 5a is ascribed to O_2 desorption from supported Pd oxo species, since an analogous TPD feature was not observed for the $MgAlO_x$ support (Fig. 1a) and a qualitatively similar TPD trace (Fig. 5b) was obtained from an oxygen-pretreated Pd/$MgAlO_x$ catalyst that had not been exposed to NO_2. For comparison, the TPD results of Ogata et al. [22] show that the onset of O_2 evolution from an oxygen-pretreated 5% Pd/MgO catalyst occurs at approximately 550 °C.

After the initial TPD experiment, the Pd/$MgAlO_x$ catalyst was reduced in H_2 at 500 °C, purged with He at 500 °C for 30 min, and subjected to a second NO_2 adsorption-TPD cycle at 300 °C. Comparison of the NO TPD traces (Fig. 6) reveals that the peak temperature after the second cycle is ~25 °C lower and the peak area is smaller. Quantitative analysis of the data (Table 1) indicates a lower NO_2 adsorption capacity (by ~25%) and a higher NO/O_2 ratio for the reduced catalyst relative to the oxygen-pretreated Pd/$MgAlO_x$ catalyst. The NO/O_2 ratio (1.80)

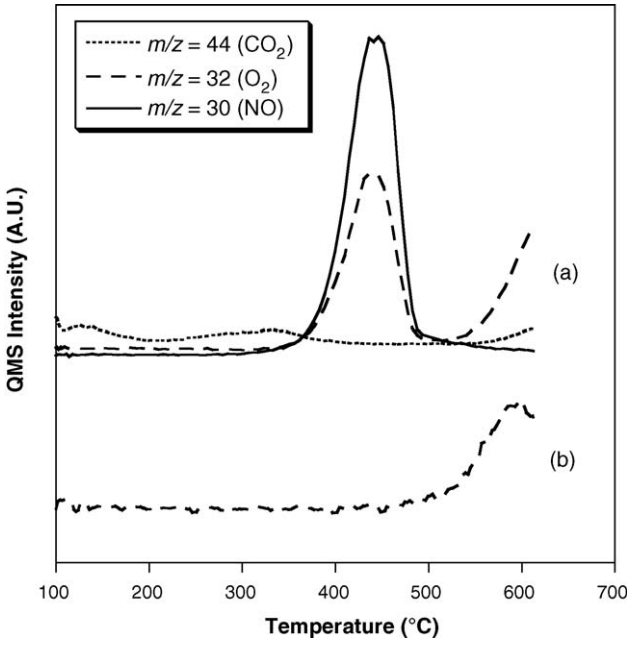

Fig. 5. TPD traces: oxygen-pretreated Pd/$MgAlO_x$ catalyst after exposure to NO_2 at 300 °C for 30 min (a) and oxygen-pretreated Pd/$MgAlO_x$ catalyst (b).

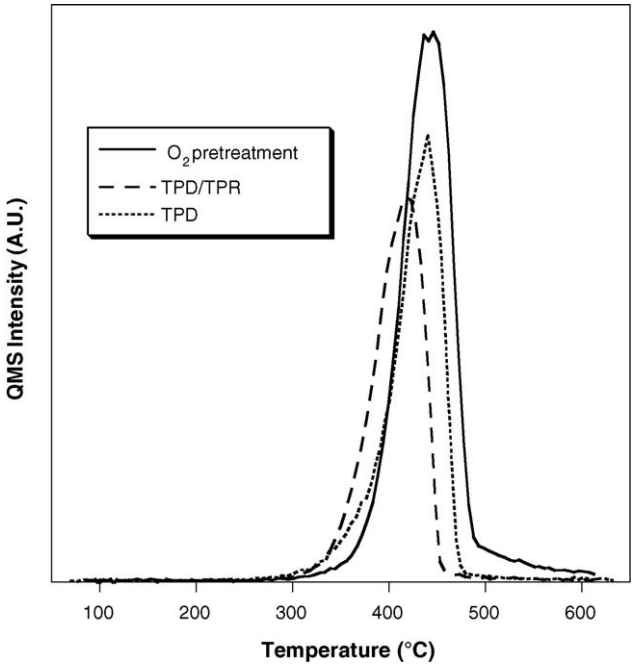

Fig. 6. Comparison of NO (m/z = 30) TPD traces for a Pd/$MgAlO_x$ catalyst. A series of NO_2 adsorption-TPD cycles was performed; the previous treatment step is indicated in the legend.

is consistent with a mixture of nitrite and nitrate surface species. For comparison, a fresh Pd/MgAlO$_x$ catalyst that had been pretreated in H_2 at 500 °C gave equivalent NO_2 adsorption-TPD results. After the second TPD cycle, the original sample was cooled in He to 300 °C, and a third NO_2 adsorption-TPD cycle was performed. The resultant NO TPD peak (Fig. 6) appears at higher temperature (~440 °C), and there is a modest increase in NO_2 adsorption capacity and a decrease in NO/O_2 ratio—partially reversing the trends observed after TPR of the Pd/MgAlO$_x$ catalyst.

In a second series of adsorption-TPD experiments, an oxygen-pretreated Pd/MgAlO$_x$ catalyst was exposed to a gas mixture containing 500 ppm NO, 500 ppm N_2 and 5% O_2 at 300 °C, and a QMA was used to monitor the uptake of NO and evolution of gaseous products during the 30 min exposure time. N_2 serves as an inert tracer and QMA calibration standard in these experiments provided that it is not adsorbed (or desorbed) by the catalyst. The temporal QMA response to a step increase in NO + O_2 concentration is shown in Fig. 7a. The N_2 signal initially rises sharply and then slowly declines toward a steady-state (SS) value of approximately 4.4×10^{-9} Torr. The slight overshoot suggests that N_2 may be a secondary product of NO adsorption on the catalyst. The NO signal rises more slowly and asymptotically approaches a SS value of approximately 3.9×10^{-9} Torr. After signal calibration, the NO uptake was estimated using the difference in area between the NO trace and an ideal step response (Table 1). The H_2O signal shows an initial peak that coincides with NO uptake by the catalyst and then declines toward a SS value. The N_2O signal ($m/z = 44$) also shows a small initial increase above the background level for this gas mixture. The $m/z = 46$ response is flat indicating that NO_2 is not produced in a detectable effluent concentration over the Pd/MgAlO$_x$ catalyst under these conditions. The NO uptake by the MgAlO$_x$ support during NO + O_2 exposure at 300 °C was measured and is included in Table 1 for comparison.

The TPD traces in Fig. 7b were recorded after an oxygen-pretreated Pd/MgAlO$_x$ catalyst was exposed NO + O_2 at 300 °C for 30 min. The dominant TPD features are concurrent NO and O_2 peaks at 415 °C and a second O_2 desorption peak at 600 °C. The corresponding NO_x adsorption capacity and NO/O_2 ratio are given in Table 1. The adsorption capacity measured by TPD is almost a factor of 2 lower than for NO_2 adsorption on an oxygen-pretreated Pd/MgAlO$_x$ catalyst. The NO/O_2 ratio (1.25) is consistent with the decomposition of surface nitrate species. The large O_2 TPD peak at 600 °C is consistent with desorption from supported Pd oxo species.

The temporal QMA response characterizing NO + O_2 adsorption on a reduced Pd/MgAlO$_x$ catalyst is shown in Fig. 8a. The sample was an oxygen-pretreated Pd/MgAlO$_x$ catalyst that was exposed to NO + O_2 at 300 °C, subsequently reduced in H_2 at 500 °C, and purged with He. Approximately 90% NO conversion is obtained during the first 3 min on stream; thereafter, the NO signal asymptotically approaches a SS value of approximately 3.9×10^{-9} Torr. The N_2 signal jumps up initially and then decays very slowly. The expected SS N_2 partial pressure is approximately 4.4×10^{-9} Torr in the absence of N_2 generation by the catalyst. The calculated NO

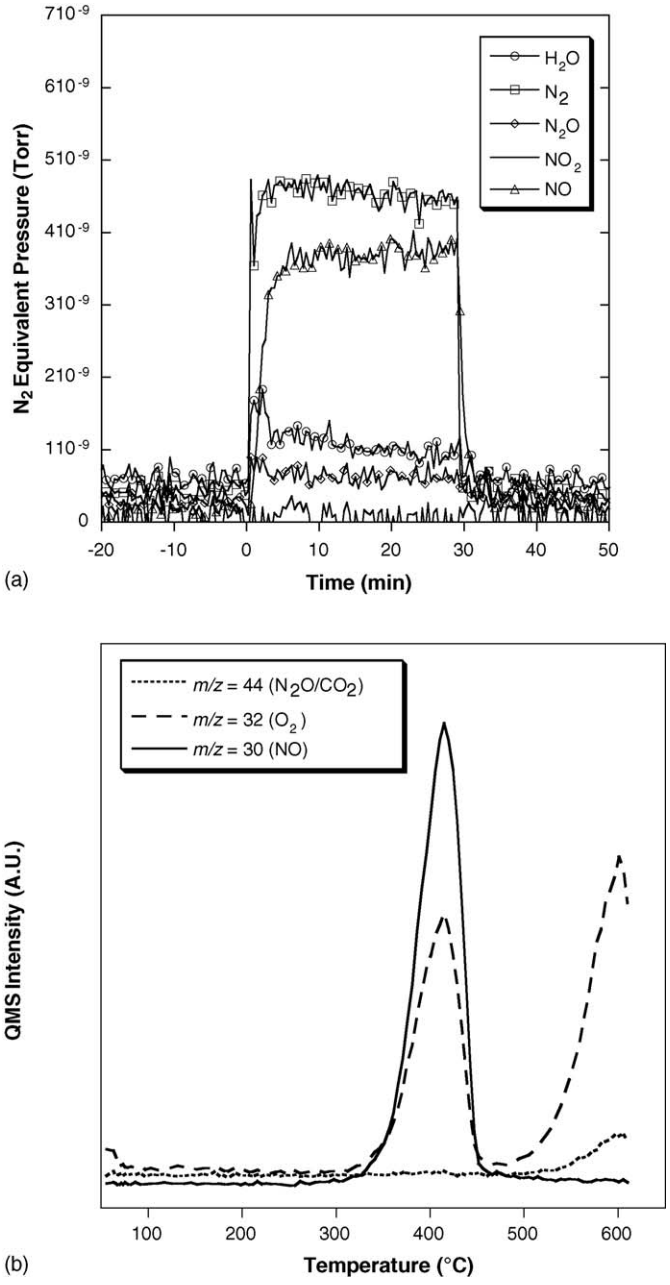

Fig. 7. (a) NO adsorption on an oxygen-pretreated Pd/MgAlO$_x$ catalyst at 300 °C. Temporal QMA response to a step increase in NO + O_2 concentration. (b) TPD traces recorded after an oxygen-pretreated Pd/MgAlO$_x$ catalyst was exposed to NO + O_2 at 300 °C for 30 min.

uptake is more than two times larger than for the oxygen-pretreated Pd/MgAlO$_x$ catalyst, and qualitatively, the amount of N_2 evolved is proportionally larger (Table 1). A relatively large quantity of H_2O is desorbed concomitant with NO uptake by the catalyst. This H_2O could be produced by NO_x reduction, but it also could arise from O_2 reduction. Although we do not know the reaction pathway by which it is produced, the hydrogen atoms must have originated on the catalyst surface, and spilled-over hydrogen from the preceding TPR step is a likely source. N_2O evolution is also observed coincident with NO + O_2 exposure. The NO_2 signal, however, remains flat indicating that the NO oxidation activity is low under these conditions. A

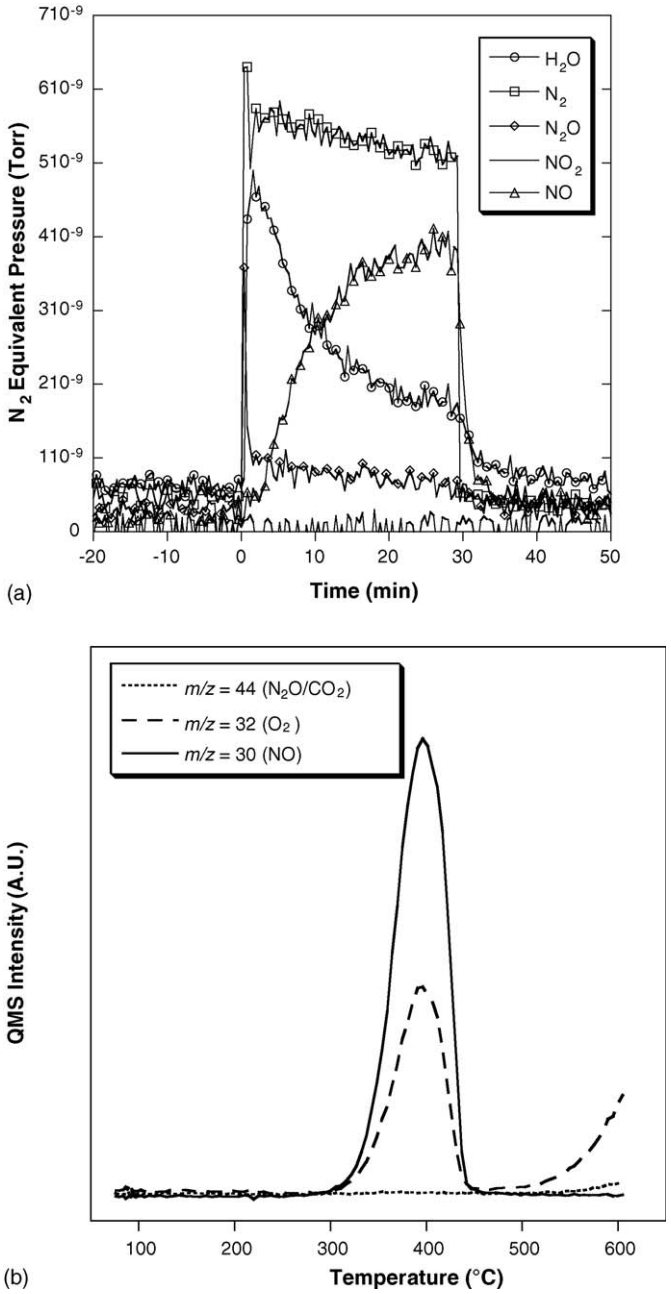

Fig. 8. (a) NO adsorption on a reduced Pd/MgAlO$_x$ catalyst at 300 °C. Temporal QMA response to a step increase in NO + O$_2$ concentration. (b) TPD traces recorded after a reduced Pd/MgAlO$_x$ catalyst was exposed to NO + O$_2$ at 300 °C for 30 min.

recent investigation found that a Pd/Ba/Al$_2$O$_3$ catalyst was significantly less active than Pt/Ba/Al$_2$O$_3$ for NO oxidation at 300 °C under lean conditions, although the Pd-containing catalyst had a greater NO$_x$ storage capacity [8].

The TPD traces in Fig. 8b were recorded after NO + O$_2$ adsorption on the reduced Pd/MgAlO$_x$ catalyst. The large NO and O$_2$ peaks at 395 °C are assigned to the decomposition of adsorbed NO$_x$ species. The corresponding NO$_x$ storage capacity and NO/O$_2$ ratio are given in Table 1. The NO$_x$ storage capacity of the reduced Pd/MgAlO$_x$ catalyst for NO + O$_2$ (as measured by TPD) is a factor of 2 higher than for the oxidized Pd/MgAlO$_x$ catalyst, consistent with the NO uptake measurements. The data suggest that metallic Pd particles are more efficient than Pd oxo species in catalyzing the conversion and storage of NO as surface nitrates and nitrites under lean conditions. As expected, high-temperature O$_2$ desorption is diminished relative to the oxygen-pretreated Pd/MgAlO$_x$ catalyst. Unfortunately, the increased NO$_x$ storage capacity of the reduced catalyst is lost after TPD, as indicated in Table 1. This may be due to Pd sintering, as suggested by the XPS results below.

The XP spectrum of a hydrogen-pretreated Pd/MgAlO$_x$ catalyst after exposure to 500 ppm NO + 5% O$_2$ at 300 °C for 30 min is shown in Fig. 4c. The spectrum is similar to that of the oxygen-pretreated catalyst (Fig. 4b); however, the Pd 3d$^{5/2}$ binding energy is slightly lower (E_b = 335.9 eV), and there is a barely perceptible shoulder at a lower binding energy consistent with metallic Pd. This spectrum is consistent with a mixture of Pd^{2+} and Pd^0 species. Salasc et al. [8] reported high-resolution XPS of a Pd/BaO/Al$_2$O$_3$ catalyst that was reduced and subsequently exposed to lean NO$_x$ storage conditions, and their Pd 3d spectra provide unequivocal evidence of both Pd^{2+} and Pd^0 species. A plausible interpretation is that surface Pd atoms are oxidized during NO$_x$ storage under lean conditions, but a core of metallic Pd remains [22]. The Pd 3d XP spectrum in Fig. 4d was measured after a NO + O$_2$ adsorption-TPD cycle on a hydrogen-pretreated Pd/MgAlO$_x$ catalyst. The 3d$^{5/2}$ binding energy (334.7 eV) is indicative of metallic Pd, and the lower intensity of the peaks (relative to Fig. 4a) suggests sintering of the supported Pd particles.

The TPR traces in Fig. 9a were measured after a hydrogen-pretreated Pd/MgAlO$_x$ catalyst was exposed to 500 ppm NO$_2$, 10% CO$_2$ and 6% O$_2$ (bal. He) at 300 °C for 30 min. The NO and O$_2$ desorption peaks typically observed during TPD are

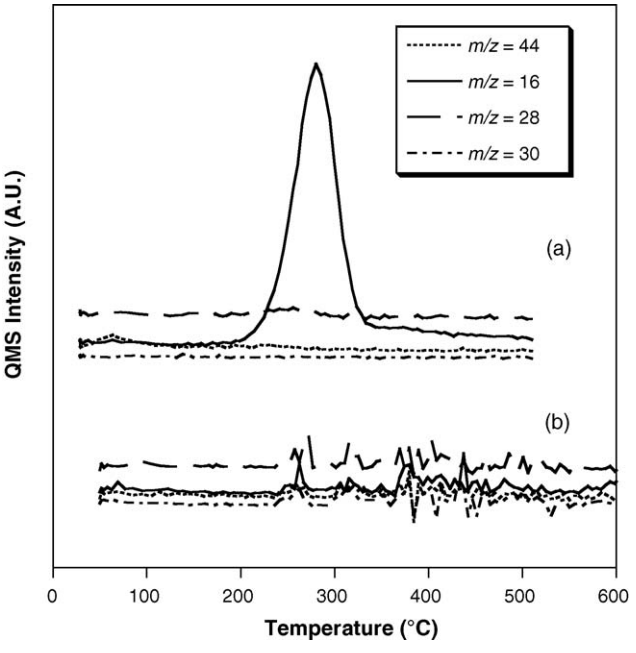

Fig. 9. TPR traces recorded after exposure of a Pd/MgAlO$_x$ catalyst to NO$_2$ (a) and NO + O$_2$ (b) at 300 °C for 30 min.

absent, indicating that the adsorbed NO_x species have been removed; however, the TPR traces do not contain any peaks due to nitrogen-containing reduction products (N_2, N_2O or NH_3). Instead, only a sharp $m/z = 16$ peak due to CH_4 evolution is observed at 320 °C. Assignment of this TPR peak to CH_4 (and not NH_3) was established by examining the electron impact fragmentation pattern in the QMA. We infer that CH_4 must originate from adsorbed CO_2, as there was no other carbon source in these experiments. The TPR traces in Fig. 9b were measured after $NO + O_2$ adsorption on a Pd/$MgAlO_x$ catalyst; there are no significant peaks which supports our assignment of the TPR peak in Fig. 9a to CO_2-derived CH_4. The TPR results were replicated several times using Pd/$MgAlO_x$ catalysts with a variety of treatment histories. The TPR data suggest that NO_x species adsorbed on the Pd/$MgAlO_x$ catalyst are reduced by H_2 prior to the start of the temperature ramp (i.e., at ∼50 °C). H_2 has been shown to be more effective than CO or propylene as a reducing agent for adsorbed NO_x species on Pt/BaO/Al_2O_3 NSR catalysts [23,24]. The very low reduction temperature inferred here may result from the close proximity of the adsorbed NO_x species to the Pd sites.

4. Summary and conclusions

NO_2 adsorption on the $MgAlO_x$ support produces primarily surface nitrate species that decompose thermally to $NO + O_2$ at 400–500 °C. The adsorbed NO_x species are reduced to N_2 at lower temperatures (300–400 °C) in flowing H_2. The adsorption capacity of the support for $NO + O_2$ is much lower, and the NO/O_2 ratio in subsequent TPD is consistent with a mixture of nitrite and nitrate surface species. The oxygen-pretreated Pd/$MgAlO_x$ catalyst exhibits 70% greater NO_2 adsorption capacity than the $MgAlO_x$ support indicating that Pd oxo species provide additional adsorption sites. The NO_2 adsorption capacity and stoichiometry of the adsorbed NO_x species are influenced by the treatment history of the Pd/$MgAlO_x$ catalyst. The average NO/O_2 ratio in TPD varies from 1.1 to 1.8 depending on the initial Pd oxidation state.

The adsorption capacity of the oxygen-pretreated Pd/$MgAlO_x$ catalyst for $NO + O_2$ at 300 °C is almost four-fold greater than $MgAlO_x$ evidencing a catalytic role of Pd in the NO_x storage mechanism. The $NO + O_2$ storage capacity and TPD NO/O_2 ratio for the oxygen-pretreated Pd/$MgAlO_x$ catalyst are equivalent (within experimental uncertainty) to those characterizing NO_2 adsorption on the $MgAlO_x$ support. Hydrogen pretreatment of the Pd/$MgAlO_x$ catalyst results in greater $NO + O_2$ adsorption capacity; however, the effect is not permanent. The $NO + O_2$ storage capacity of the oxygen-pretreated catalyst and the reduced catalyst after an adsorption-TPD cycle are equivalent. The ratio of NO uptake to NO desorbed during TPD is approximately 3:1 for $MgAlO_x$ and the Pd/$MgAlO_x$ catalyst regardless of its treatment history. TPR experiments indicate that the surface species formed by adsorption of either NO_2 or $NO + O_2$ on the Pd/$MgAlO_x$ catalyst are removed in flowing H_2 at very low temperatures (∼50 °C).

Acknowledgments

This work was supported by Caterpillar, Inc. and the U.S. Department of Energy. XRD measurements were performed in Prof. James Martin's laboratory in the NCSU Chemistry Department.

References

[1] R.M. Heck, R.J. Farrauto, Catalytic Air Pollution Control, Wiley, New York, 2002.
[2] N. Takahashi, H. Shinjoh, T. Iijima, T. Suzuki, K. Yamazaki, K. Yokota, H. Suzuki, N. Miyoshi, S. Matsumoto, T. Tanizawa, T. Tanaka, S. Tateishi, K. Kasahara, Catal. Today 27 (1996) 63.
[3] W.S. Epling, L.E. Campbell, A. Yezerets, N.W. Currier, J.E. Parks, Catal. Rev.-Sci. Eng. 46 (2004) 163.
[4] E. Fridell, H. Persson, B. Westerberg, L. Olsson, M. Skoglundh, Catal. Lett. 66 (2000) 71.
[5] F. Prinetto, G. Ghiotti, I. Nova, L. Lietti, E. Tronconi, P. Forzatti, J. Phys. Chem. B 105 (2001) 12732.
[6] D. Uy, K.A. Wiegand, A.E. O'Neill, M.A. Dearth, W.H. Weber, J. Phys. Chem. B 106 (2002) 387.
[7] C. Sedlmair, K. Seshan, A. Jentys, J.A. Lercher, Catal. Today 75 (2002) 413.
[8] S. Salasc, M. Skoglundh, E. Fridell, Appl. Catal. B 36 (2002) 145.
[9] G. Fornasari, F. Trifiro, A. Vaccari, F. Prinetto, G. Ghiotti, G. Centi, Catal. Today 75 (2002) 421.
[10] H.W.F. Taylor, Miner. Mag. 39 (1973) 377.
[11] D. Tichit, B. Coq, Catal. Tech. 7 (2003) 206.
[12] F. Prinetto, M. Manzoli, G. Ghiotti, M. deJ.M. Ortiz, D. Tichit, B. Coq, J. Catal. 222 (2004) 238.
[13] X. Wang, S.M. Sigmon, J.J. Spivey, H.H. Lamb, Catal. Today 96 (2004) 11.
[14] B.A. Silletti, Masters Thesis, North Carolina State University, Raleigh, NC, 2004.
[15] S. Miyata, Clay Miner. 28 (1980) 50.
[16] K.J.D. MacKenzie, R.H. Meinhold, B.L. Sherriff, Z. Xu, J. Mater. Chem. 3 (1993) 1263.
[17] J. Shen, J.M. Kobe, Y. Chen, J.A. Dumesic, Langmuir 10 (1994) 3902.
[18] K.I. Hadjiivanov, Catal. Rev.-Sci. Eng. 42 (2000) 71.
[19] J.A. Rodriguez, T. Jirsak, S. Sambasivan, D. Fischer, A. Maiti, J. Chem. Phys. 112 (2000) 9929.
[20] C. Pazé, G. Gubitosa, S. Orso Giacone, G. Spoto, F.X. Llabrés i Xamena, A. Zecchina, Top. Catal. 30/31 (2004) 169.
[21] W.F. Schneider, J. Phys. Chem. B 108 (2004) 273, and references therein.
[22] A. Ogata, A. Obuchi, K. Mizuno, H. Aoyama, H. Ohuchi, J. Catal. 144 (1993) 452.
[23] H. Mahzoul, P. Gilot, J.-F. Brilhac, B.R. Stanmore, Top. Catal. 16/17 (2001) 293.
[24] S. Poulston, R.R. Rajaram, Catal. Today 81 (2003) 603.